Malaysian Journal of Mathematical Sciences 14(1): 139–168 (2020)

MALAYSIAN JOURNAL OF MATHEMATICAL SCIENCES

Journal homepage: http://einspem.upm.edu.my/journal

Numerical Solution of Space-time Variable Fractional Order Advection-Dispersion Equation using Jacobi Spectral Collocation Method

Soltanpour Moghadam, A.[1], Arabameri, M. *[2], Barfeie, M.[3], and Baleanu, D.[4]

[1] *Department of Mathematics, University of Sistan and Baluchestan, Zahedan, Iran*
[2] *Department of Mathematics, University of Sistan and Baluchestan, Zahedan, Iran*
[3] *Department of Mathematics, Sirjan University of Technology, Sirjan, Iran*
[4] *Department of Mathematics, Faculty of Art and Sciences, Cankaya University, Balgat 06530, Ankara, Turkey and Institute of Space Sciences, Magurele-Bucharest, Romania*

E-mail: arabameri@math.usb.ac.ir
* *Corresponding author*

Received: 8 April 2019
Accepted: 27 December 2019

ABSTRACT

This article is aimed at studying computational solution of variable order fractional advection-dispersion equation for one-dimensional and two-dimensional spaces utilizing spectral collocation method. In the considered model, the time derivative is Coimbra fractional derivative and space derivative is a Riemann-Liouville derivative. Jacobi polynomials are applied as basic functions in approximation of the solution. The presented approach is an application of the shifted Jacobi-Gauss collocation (SJ-G-C) and the shifted Jacobi-Gauss-Radau collocation (SJ-GR-C) methods using for discretizing along space and time, respectively. Using the related collocation points, the problem would be changed to an algebraic equation system, which can be tackled applying a computational technique. At the end, several examples in one and two dimensional cases have been solved by introduced approach, it would be shown that the proposed numerical algorithm has considerably higher accuracy in contrast to the existing computational schemes including finite difference approach.

Keywords: Advection-dispersion equation, Fractional derivative of variable-order, Shifted Jacobi polynomials.

1. Introduction

Differential equations of fractional type have several applications in the various fields of science and engineering. They have significantly grown in recent years Chen et al. (2014), Hosseini et al. (2017), Magin (2006), Ortega et al. (2018), Sakar and Güney (2017), Sontakke et al. (2018), Ünal and Gökdoğan (2017). Some works have been done on analytical solution of these equations Pandey et al. (2011). However, the analytical solution of such equations cannot be furnished due to non-locality feature of fractional derivatives, thus numerical solution of these equations is of great importance. We will focus on fractional advection-dispersion equation (FADE) in this article Schumer et al. (2001), Zhang et al. (2007). FADEs are used to model most sciences of physics, chemical engineering, and geology including the description of heat transfer in film draining Isenberg and Gutfinger (1973), porous media flow Kumar (1983), transfer of mass Guvanasen and Volker (1983), water transport in soils Parlange (1980), transport of pollutants in rivers and streams Chatwin and Allen (1985), Clavero et al. (2003), thermal pollution in river system Chaudhry et al. (1983) and etc.

Several methods have been suggested to obtain analytical and numerical solutions of these equations. Pandey et al. (2011) proposed a theoretic scheme via the analytic method of homotopy for FADEs. Meerschaert and Tadjeran (2004) implemented an Euler method of implicit type via improved Grunwald estimation for FADEs and showed that the approach is compatible and unconditionally stable. Furthermore, some other schemes were presented to approximate FADE solutions like finite difference Liu et al. (2007), finite element Ervin and Roop (2006), finite volume Hejazi et al. (2014), and spectral approaches Carella and Dorao (2013), Zheng and Wei (2010). Operators of FADE's fractional derivative are in terms of space and time, which the order can be fixed or variable. The variable order fractional differential operator is a natural candidate for presenting a fruitful mathematical framework for describing complicated dynamic problems Gómez-Aguilar (2018), Sun et al. (2009), Tseng (2006). The following FADE with space-time variable order would be surveyed in this study

$$\begin{aligned} D_t^{\xi(x,y)} f(x,y,t) =& \vartheta({}_0^R D_x^{\eta_1(x,y,t)} f(x,y,t) + {}_0^R D_y^{\eta_2(x,y,t)} f(x,y,t)) \\ &- \kappa({}_0^R D_x^{\rho_1(x,y,t)} f(x,y,t) + {}_0^R D_y^{\rho_2(x,y,t)} f(x,y,t)) \\ &+ S(f,x,y,t), \qquad (x,y,t) \in [0,L] \times [0,I] \times [0,T], \end{aligned} \tag{1}$$

wherein the initial and boundary conditions are defined by

$$f(x,y,0) = \varphi_1(x,y), \qquad (x,y) \in \Omega = [0,L] \times [0,I], \tag{2}$$

$$f(x,y,t)=\varphi_2(x,y,t), \qquad (x,y)\in\partial\Omega,\ t\in[0,T], \tag{3}$$

wherein $\vartheta,\kappa>0$, $0<\underline{\xi}\le\xi(x)\le\overline{\xi}\le 1$, $1<\underline{\eta}\le\eta_1,\eta_2\le\overline{\eta}\le 2$ and $0<\underline{\rho}\le\rho_1,\rho_1\le\overline{\rho}\le 1$. Here $\partial\Omega$ is the boundary of Ω, and $\varphi_1$and φ_2 of the functions are smooth enough. In addition, fractional derivatives of time and space are of Coimbra Coimbra (2003) and Riemann-Liouville Zhuang et al. (2009) types, respectively. Also one dimensional FADE can be easily deduced through equation (1).

This article proposes a numerical solution method for variable-order fractional advection-dispersion equations (VO-FADEs). A VO-FADE might contain partial differential operators whose orders can be functions in the time and space variables. The solutions of VO-FADEs are complicated in general, and they are not given in practice. Therefore, to construct accurate and efficient numerical solution methods for VO-FADEs is an important task. Zhang et al. (2014) presented an Euler scheme of implicit type to tackle these equations in one-dimensional state and they obtained results of reasonable accuracy using considerable number of points.

Spectral methods are powerful tools for tackling different types of differential equations, Atabakan et al. (2014), Bhrawy and Zaky (2015), Bhrawy and Alghamdi (2012), Canuto et al. (2006), Eslahchi et al. (2014). Spectral collocation scheme has increasingly been used to tackle differential equations of fractional type Bhrawy et al. (2016a,b, 2015). Two attributes of *exponential convergence* and *ease of use* have led the researchers to tend to this method. Special types of this method, which are more applicable and widely used, are Galerkin, tau Ahmadian et al. (2017), and collocation methods.

In the study, a spectral algorithm would be used to discretize space and time in order to provide a highly accurate numerical solution for FADEs in one-dimensional and two-dimensional cases. Moreover, we will reveal that the obtained results are far more accurate compared to the findings provided by Zhang et al. Jacobi-Gauss colocation method will be utilized to solve FADEs in this study. The major step to this approach is considering the solution as a series of shifted Jacobi polynomials Ahmadian et al. (2016) with unknown coefficients. These coefficients are selected so that the FADE remainder would be zero at collocation points. Our purpose in applying shifted Jacobi polynomials, $P_j^{(\omega,\varrho)}(z)$ $(j\ge 0,\omega,\varrho>-1)$, in addition to the orthogonal properties of these polynomials is to obtain an approximate solution based on Jacobi parameters ω and ϱ and by changing these parameters we can use ultra-spherical, shifted Chebyshev of the 1st and 2nd types, shifted Legendre and the third and fourth kinds of the shifted Chebyshev polynomials (see Remark 2.1).

Here, a mixed collocation method will be used to discretize along time and space. To be more precise, shifted Jacobi-Gauss and shifted Jacobi-Gauss-Radau collocation schemes are used to discretize the spatial and temporal variables, respectively Canuto et al. (2006). Finally, through implementing collocation method on FADE and boundary and initial conditions, an equation system is constructed, that could be easily resolved with a classic numerical technique and the unknown coefficients would be subsequently attained. At the end, various FADEs with fractional and fixed order derivative would be solved in 1D and 2D cases and highly accurate solutions would be furnished for these problems.

The remaining parts of this work will be provided as follows. In Section 2, a preliminaries to the notions of Riemann-Liouville and Coimbra fractional derivatives as well as basic concepts of Jacobi polynomials would be mentioned. Spectral collocation method for discretizing space and time variables in advection-dispersion equation in 1D and 2D states is brought forward in Section 3. The numerical experiment for indicating high precision and efficiency of the presented technique in contrast to the other approaches have been presented in section 4. Finally, a summary of the presented scheme will be stated in Section 5.

2. Preliminaries

In this part, firstly, variable order fractional derivatives in equation (1) would be defined. Then, definitions of shifted Jacobi polynomials and their fractional derivatives will be provided.

2.1 Fractional derivatives definitions

Definition 2.1. *Coimbra Coimbra (2003) fractional differential operator with variable order of $\xi(x)$ is given as follows when $0 < \xi(x) \leq 1$:*

$$D_t^{\xi(x)} f\left(x,t\right) = \frac{1}{\Gamma\left(1-\xi(x)\right)} \int_{0^+}^{t} \left(t-\sigma\right)^{-\xi(x)} \frac{\partial f(x,\sigma)}{\partial \sigma} d\sigma + \frac{\left(f\left(x,0^+\right)-f(x,0^-)\right) t^{-\xi(x)}}{\Gamma\left(1-\xi(x)\right)}, \tag{4}$$

wherein $\Gamma\left(\cdot\right)$ shows function of Euler Gamma.

Suppose that $f \in C^2(\Omega)$, we will survey the solution $f(x,t)$ for $t \geq 0$. As a result, it is considered that this characteristic of $f(x,t)$ in $t=0$ is good enough, thus in the case of $f(x,0^+) = f(x,0^-)$ in the Coimbra fractional operator definition, the operator would be correspondent to the well-known Caputo fractional operator in Sun et al. (2012), Zhuang et al. (2009).

Definition 2.2. *Variable-order fractional differential operator of Riemann-Liouville Zhuang et al. (2009) from $\eta(x,t)$ order is defined by:*

$$ {}_0^R D_x^{\eta(x,t)} f(x,t) = \left[\frac{1}{\Gamma(m-\eta(x,t))} \frac{d^m}{d\sigma^m} \int_0^{\sigma} (\sigma-\delta)^{m-\eta(x,t)-1} f(\delta,t)\, d\delta \right]_{\sigma=x}, \tag{5} $$

where $m-1 < \eta(x,t) \leq m$.

2.2 Jacobi polynomials (JP)

We will introduce the Jacobi polynomials in this subsection. Jacobi polynomials is denoted by $P_j^{(\omega,\varrho)}(z)$, $(j = 0,1,\ldots)$ where $\omega, \varrho > -1$ creates an orthogonal system on interval of $[-1,1]$ in terms of the function of weight $w^{(\omega,\varrho)}(z) = (1-z)^{\omega}(1+z)^{\varrho}$ Szeg (1939). In other words:

$$ \left(P_k^{(\omega,\varrho)}(z), P_l^{(\omega,\varrho)}(z) \right)_{w^{(\omega,\varrho)}} = \int_{-1}^{1} P_k^{(\omega,\varrho)}(z)\, P_l^{(\omega,\varrho)}(z)\, w^{(\omega,\varrho)}(z)\, dz = h_k^{(\omega,\varrho)} \delta_{lk}, \tag{6} $$

where δ_{lk} is the Kronecker function and

$$ h_k^{(\omega,\varrho)} = \frac{2^{(\omega+\varrho+1)} \Gamma(k+\omega+1)\, \Gamma(k+\varrho+1)}{(2k+\omega+\varrho+1) k! \Gamma(k+\omega+\varrho+1)}. \tag{7} $$

Also $P_i^{(\omega,\varrho)}(z)$, $(i = 0,1,\ldots)$ can be written through the recursive relations below Askey (1975):

$$ \begin{aligned} &P_{i+1}^{(\omega,\varrho)}(z) = \left(a_i^{(\omega,\varrho)} z - b_i^{(\omega,\varrho)} \right) P_i^{(\omega,\varrho)}(z) - c_i^{(\omega,\varrho)} P_{i-1}^{(\omega,\varrho)}(z), \quad i \geq 1, \\ &P_0^{(\omega,\varrho)}(z) = 1, P_1^{(\omega,\varrho)}(z) = \frac{1}{2}(\omega+\varrho+2) z + \frac{1}{2}(\omega-\varrho), \end{aligned} \tag{8} $$

wherein

$$a_i^{(\omega,\varrho)} = \frac{(2i+\omega+\varrho+1)\,(2i+\omega+\varrho+2)}{2\,(i+1)\,(i+\omega+\varrho+1)}, \tag{9}$$

$$b_i^{(\omega,\varrho)} = \frac{(2i+\omega+\varrho+1)(\varrho^2-\omega^2)}{2(i+1)(i+\omega+\varrho+1)(2i+\omega+\varrho)}, \tag{10}$$

$$c_i^{(\omega,\varrho)} = \frac{(2i+\omega+\varrho+2)\,(i+\omega)\,(i+\varrho)}{(i+1)\,(i+\omega+\varrho+1)\,(2i+\omega+\varrho)}. \tag{11}$$

2.3 Shifted Jacobi polynomials (SJP)

Shifted Jacobi polynomials $P_{L,i}^{(\omega,\varrho)}(x)$ in the interval of $[0,L]$ are furnished by change of variable $z = \frac{2x}{L} - 1$ in the recurrence functions (8). Therefore, the orthogonality condition (6) for the shifted Jacobi polynomials would be changed as $w_L{}^{(\omega,\varrho)}(x) = (L-x)^{\omega} x^{\varrho}$ and $h_{L,k}^{(\omega,\varrho)} = (\frac{L}{2})^{\omega+\varrho+1} h_k^{(\omega,\varrho)}$. Furthermore, the recurrence relations (8) would be written as follows:

$$\begin{aligned} &P_{L,i+1}^{(\omega,\varrho)}(x) = \left(a_i^{(\omega,\varrho)}\left(\frac{2x}{L}-1\right) - b_i^{(\omega,\varrho)}\right) P_{L,i}^{(\omega,\varrho)}(x) - c_i^{(\omega,\varrho)} P_{L,i-1}^{(\omega,\varrho)}(x), \\ &P_{L,0}^{(\omega,\varrho)}(x) = 1, P_{L,1}^{(\omega,\varrho)}(x) = \frac{1}{L}(\omega+\varrho+2)\,x - (\varrho+1), \end{aligned} \tag{12}$$

where $P_{L,i}^{(\omega,\varrho)}(x) = P_i^{(\omega,\varrho)}\left(\frac{2x}{L}-1\right)$.

Remark 2.1. *SJPs include an infinite number of orthogonal polynomials such as shifted ultra-spherical polynomials (ω=ϱ), shifted Chebyshev polynomials of the 1st and 2nd types (ω=ϱ= $\pm\frac{1}{2}$), shifted Legendre polynomials (ω=ϱ= 0), and the third and fourth kinds of the shifted Chebyshev polynomials (ω= $-\varrho$= $\pm\frac{1}{2}$).*

For the shifted Jacobi polynomials $P_{L,i}^{(\omega,\varrho)}(x)$ we have

$$\begin{aligned} P_{L,i}^{(\omega,\varrho)}(x) &= \sum_{s=0}^{i} (-1)^{i+s} \frac{\Gamma(i+\varrho+1)\,\Gamma(i+s+\omega+\varrho+1)}{\Gamma(s+\varrho+1)\,\Gamma(i+\omega+\varrho+1)\,(i-s)!s!L^s} x^s \\ &= \sum_{s=0}^{i} \frac{\Gamma(i+\varrho+1)\,\Gamma(i+s+\omega+\varrho+1)}{\Gamma(s+\omega+1)\,\Gamma(i+\omega+\varrho+1)\,(i-s)!s!L^s} (x-L)^s. \end{aligned} \tag{13}$$

Also, the SJPs end point values are specified as follows:

$$P_{L,i}^{(\omega,\varrho)}(0) = (-1)^i \frac{\Gamma(i+\varrho+1)}{\Gamma(\varrho+1)\,i!}, \qquad P_{L,i}^{(\omega,\varrho)}(L) = \frac{\Gamma(i+\omega+1)}{\Gamma(\omega+1)\,i!}. \tag{14}$$

Jacobi-Gauss quadrature is used for accurate assessment of integral in relation (6). For each $\phi\in S_{2N+1}[0,L]$, we have:

$$\int_0^L \phi\left(x\right) w_L^{(\omega,\varrho)}\left(x\right) dx = \sum_{j=0}^{N} \varpi_{G,L,j}^{(\omega,\varrho)} \phi\left(x_{G,L,j}^{(\omega,\varrho)}\right), \tag{15}$$

where $S_N[0,L]$ is a collection of polynomials of degrees less or equal than N. In addition, $x_{G,L,j}^{(\omega,\varrho)}$ for any $(0 \leq j \leq N)$ and $\varpi_{G,L,j}^{(\omega,\varrho)}$ for any $(0 \leq j \leq N)$ are correspondent nodes and Christoffel numbers in $[0,L]$ interval, respectively. For SJ-G quadrature, $x_{G,L,j}^{(\omega,\varrho)}$ are zeros of $P_{L,N+1}^{(\omega,\varrho)}\left(x\right)$ and the weights are as follows:

$$\varpi_{G,L,j}^{(\omega,\varrho)} = \frac{C_{L,N}^{(\omega,\varrho)}}{(L - x_{G,L,j}^{(\omega,\varrho)}) x_{G,L,j}^{(\omega,\varrho)} [\partial_x P_{N+1}^{(\omega,\varrho)}(x_{G,L,j}^{(\omega,\varrho)})]^2}, \tag{16}$$

where

$$C_{L,N}^{(\omega,\varrho)} = \frac{L^{(\omega+\varrho+1)}\Gamma\left(N+\omega+2\right)\Gamma\left(N+\varrho+2\right)}{(N+1)!\Gamma\left(N+\omega+\varrho+2\right)}. \tag{17}$$

Furthermore, for the SJ-GR quadrature, $x_{R,L,j}^{(\omega,\varrho)}$ are zeros of $P_{L,N}^{(\omega,\varrho+1)}\left(x\right)$ and $x_{R,L,0}^{(\omega,\varrho)} = 0$ and the weights are as follows:

$$\varpi_{R,L,0}^{(\omega,\varrho)} = \frac{L^{(\omega+\varrho+1)}(\varrho+1)\Gamma^2(\varrho+1)\Gamma\left(N+1\right)\Gamma\left(N+\omega+1\right)}{\Gamma\left(N+\varrho+2\right)\Gamma\left(N+\omega+\varrho+2\right)}, \tag{18}$$

$$\varpi_{R,L,j}^{(\omega,\varrho)} = \frac{C_{L,N-1}^{(\omega,\varrho+1)}}{(L - x_{R,L,j}^{(\omega,\varrho)})(x_{R,L,j}^{(\omega,\varrho)})^2 \partial_x [P_N^{(\omega,\varrho+1)}(x_{R,L,j}^{(\omega,\varrho)})]^2}, \quad 1\leq j\leq N. \tag{19}$$

Suppose that $f(x)$ is the square-integrable function in terms of the Jacobi weight function of $w_L^{(\omega,\varrho)}(x)$. Therefore, this function could be provided as the shifted Jacobi polynomials in what follows:

$$f\left(x\right) = \sum_{j=0}^{\infty} \hat{a}_j P_{L,j}^{(\omega,\varrho)}\left(x\right), \tag{20}$$

wherein $\hat{a}_j$ coefficients are defined as follows:

$$\hat{a}_j = \frac{1}{h_{L,j}^{(\omega,\varrho)}} \int_0^L f\left(x\right) P_{L,j}^{(\omega,\varrho)}\left(x\right) w_L^{(\omega,\varrho)}\left(x\right) dx. \tag{21}$$

Practically, approximation of $f(x)$ can be used to cut the relation (20) into $N+1$ parts so that:

$$f(x) \simeq f_N(x) = \sum_{j=0}^{N} \hat{a}_j P_{L,j}^{(\omega,\varrho)}(x). \tag{22}$$

Similarly, an infinitely differentiable function like $f(x,t)$ with two independent variables in interval of $\Omega = [0,L] \times [0,T]$ can be written in some parts of the Shifted Jacobi polynomials as comes next:

$$f_N(x,t) = \sum_{i,j=0}^{N} \hat{a}_{ij} P_{L,i}^{(\omega_1,\varrho_1)}(x) P_{T,j}^{(\omega_2,\varrho_2)}(t), \tag{23}$$

where

$$\hat{a}_{ij} = \frac{1}{h_{T,i}^{(\omega_2,\varrho_2)} h_{L,j}^{(\omega_1,\varrho_1)}} \int_0^T \int_0^L f(x,t) P_{T,i}^{(\omega_2,\varrho_2)}(t) P_{L,j}^{(\omega_1,\varrho_1)}(x) w_T^{(\omega_2,\varrho_2)}(t) w_L^{(\omega_1,\varrho_1)}(x)\, dxdt. \tag{24}$$

and also for $f(x,y,t)$ with three independent variables in interval of $\Omega = [0,L] \times [0,I] \times [0,T]$ can be written as comes next:

$$f_N(x,y,t) = \sum_{i,j,k=0}^{N} \hat{a}_{ijk} P_{L,i}^{(\omega_1,\varrho_1)}(x) P_{I,j}^{(\omega_2,\varrho_2)}(y) P_{T,k}^{(\omega_3,\varrho_3)}(t). \tag{25}$$

2.3.1 SJP variable fractional order derivatives

The basis of our numerical method is in approximating the solution of (1) based on (25). Thus, by substituting (25) in (1), it is needed to furnish the Riemann-Liouville and Caputo derivatives of $f(x,y,t)$. We know that if $f(x) = (x-a)^n$ and $n > -1$ and $\eta > 0$, Riemann-Liouville derivative of $f(x)$ function would be derived as follows Diethelm (2010):

$${}_0^R D_a^{\eta} f(x) = \begin{cases} \frac{\Gamma(n+1)}{\Gamma(n+1-\eta)} (x-a)^{n-\eta}, & \eta - n \notin N, \\ 0, & \eta - n \in N. \end{cases} \tag{26}$$

Furthermore, for $n \geq 0$, the Caputo derivative of $f(x)$ would be furnished as follows Diethelm (2010):

$$D_x^{\xi} f(x) = \begin{cases} 0, & if\ n \in \{0,1,\ldots,m-1\}, \\ \frac{\Gamma(n+1)}{\Gamma(n+1-\xi)} (x-a)^{n-\xi}, & if\ (n \in N, n \geq m)\, or\, (n \notin N, n > m-1), \end{cases} \tag{27}$$

wherein $m = \lceil \xi \rceil$ while $\lceil \cdot \rceil$ is the ceiling function. As a result, by considering (26) and (27), the fractional derivatives with variable order of the Jacobi polynomials and subsequently the fractional derivative of $f(x,t)$ function could be deduced. Therefore, by considering the analytic form of shifted Jacobi polynomials of (13) and using (26), the Riemann-Liouville derivative of the shifted Jacobi polynomials is calculated as follows:

$$\begin{aligned} &{}_0^R D_a^{\eta(x,y,t)} P_{L,i}^{(\omega,\varrho)}(x) = P_{L,i}^{(\omega,\varrho,\eta(x,y,t))}(x) \\ &= \sum_{s=0}^{i} (-1)^{i+s} \frac{\Gamma(i+\varrho+1)\,\Gamma(i+s+\omega+\varrho+1)}{\Gamma(s+\varrho+1)\,\Gamma(i+\omega+\varrho+1)\,(i-s)!\,\Gamma(s-\eta(x,y,t)+1)\,L^s} x^{s-\eta(x,y,t)}. \end{aligned} \tag{28}$$

Likewise, the same relation can be used for $\rho(x,y,t)$ order fractional derivative. In addition, using (27), the $\xi(x,y)$ order Caputo fractional derivative is given by (when $0 < \xi(x,y) \leq 1$):

$$\begin{aligned} &D_t^{\xi(x,y)} P_{L,i}^{(\omega,\varrho)}(t) = P_{L,i}^{(\omega,\varrho,\xi(x,y))}(t) \\ &= \sum_{s=1}^{i} (-1)^{i+s} \frac{\Gamma(i+\varrho+1)\,\Gamma(i+s+\omega+\varrho+1)}{\Gamma(s+\varrho+1)\,\Gamma(i+\omega+\varrho+1)\,(i-s)!\,\Gamma(s-\xi(x,y)+1)\,T^s} t^{s-\xi(x,y)}. \end{aligned} \tag{29}$$

3. Method of Jacobi Collocation

Here, we implement a computational scheme based on Jacobi collocation method so as to tackle the advection-dispersion equation with space-time variable fractional order in the one-dimensional and two-dimensional cases. Collocation points for the temporal and spatial variables are chosen from SJ-GR and SJ-G points Canuto et al. (2006), respectively.

3.1 One-dimensional case

Advection-dispersion equation with space-time variable fractional order in the 1D case is considered as follows:

$$\begin{aligned} D_t^{\xi(x)} f(x,t) = \vartheta\, {}_0^R D_x^{\eta(x,t)} f(x,t) - \kappa\, {}_0^R D_x^{\rho(x,t)} f(x,t) + S(f,x,t), \\ (x,t) \in \Omega = [0,L] \times [0,T], \end{aligned} \tag{30}$$

with the initial condition below:

$$f(x,0) = \varphi_1(x), \tag{31}$$

and the following side conditions:

$$\begin{cases} f(0,t) = \varphi_2(t), \\ f(L,t) = \varphi_3(t), \end{cases} \tag{32}$$

such that $\vartheta, \kappa > 0$, $0 < \underline{\xi} \leq \xi(x) \leq \overline{\xi} \leq 1$, $1 < \underline{\eta} \leq \eta(x,t) \leq \overline{\eta} \leq 2$ and $0 < \underline{\rho} \leq \rho(x,t) \leq \overline{\rho} \leq 1$.

Remark 3.1. *In this problem, the boundary conditions can be implemented as Dirichlet, Neumann, or mixed. We only state the Dirichlet boundary conditions since the algorithm is similar for each of the boundary conditions.*

The approximate solution is considered as stated in subsection 2.3 based on relation (23):

$$f_N(x,t) = \sum_{i,j=0}^{N} a_{ij} P_{L,i}^{(\omega_1,\varrho_1)}(x)\, P_{T,j}^{(\omega_2,\varrho_2)}(t). \tag{33}$$

For simplicity and summarization of the initial, side criteria and the fractional derivatives of $f_N(x,t)$ in the rest of the work, the following relations are defined:

$$R_0^{i,j}(x,t) = P_{L,i}^{(\omega_1,\varrho_1)}(x)\, P_{T,j}^{(\omega_2,\varrho_2)}(t), \tag{34}$$

$$R_1^{i,j}(x,t) = P_{L,i}^{(\omega_1,\varrho_1)}(x)\, P_{T,j}^{(\omega_2,\varrho_2,\xi(x))}(t), \tag{35}$$

$$R_2^{i,j}(x,t) = P_{L,i}^{(\omega_1,\varrho_1,\eta(x,t))}(x)\, P_{T,j}^{(\omega_2,\varrho_2)}(t), \tag{36}$$

$$R_3^{i,j}(x,t) = P_{L,i}^{(\omega_1,\varrho_1,\rho(x,t))}(x)\, P_{T,j}^{(\omega_2,\varrho_2)}(t), \tag{37}$$

which in relations (34)-(37), $P_{L,i}^{(\omega,\varrho,w)}(x)$ and $P_{T,j}^{(\omega,\varrho,w)}(t)$ are w-order fractional derivatives of $P_{L,i}^{(\omega,\varrho)}(x)$ and $P_{T,j}^{(\omega,\varrho)}(t)$ functions, respectively. Now, substituting (33) in (30) and using (34)-(37), we have:

$$\sum_{i,j=0}^{N} a_{ij} R_1^{i,j}(x,t) = \vartheta \sum_{i,j=0}^{N} a_{ij} R_2^{i,j}(x,t) - \kappa \sum_{i,j=0}^{N} a_{ij} R_3^{i,j}(x,t) + S\left(\sum_{i,j=0}^{N} a_{ij} R_0^{i,j}(x,t), x, t\right). \tag{38}$$

Furthermore, numerical behavior of the boundary and initial conditions will be provided as follows:

$$\begin{cases} \sum_{i,j=0}^{N} a_{ij} R_0^{i,j}\left(x,0\right) = \varphi_1\left(x\right), \\ \sum_{i,j=0}^{N} a_{ij} R_0^{i,j}\left(0,t\right) = \varphi_2\left(t\right), \\ \sum_{i,j=0}^{N} a_{ij} R_0^{i,j}\left(L,t\right) = \varphi_3\left(t\right). \end{cases} \tag{39}$$

Now, the Jacobi collocation method is implemented to solve (38) and (39). In the Jacobi collocation scheme with shifts, the remainder of (38) in $(N-1)N$ collocation point is zero. Moreover, the initial and boundary conditions are collocated in the collocation nodes.

Substituting the nodes in (38), $(N-1)N$ algebraic equation with $(N+1)^2$ unknown values of a_{ij} would be furnished:

$$\sum_{i,j=0}^{N} a_{ij} F_1^{i,j}\left(x_{G,L,r}^{(\omega_1,\varrho_1)}, t_{R,T,\tau}^{(\omega\omega_2,\varrho_2)}\right) = S\left(\sum_{i,j=0}^{N} a_{ij} R_0^{i,j}(x_{G,L,r}^{(\omega_1,\varrho_1)}, t_{R,T,\tau}^{(\omega_2,\varrho_2)}), x_{G,L,r}^{(\omega_1,\varrho_1)}, t_{R,T,\tau}^{(\omega_2,\varrho_2)}\right), \quad r = 1,\dots,N-1, \qquad \tau = 1,\dots,N, \tag{40}$$

where

$$\begin{aligned} F_1^{i,j}\left(x_{G,L,r}^{(\omega_1,\varrho_1)}, t_{R,T,\tau}^{(\omega_2,\varrho_2)}\right) &= R_1^{i,j}\left(x_{G,L,r}^{(\omega_1,\varrho_1)}, t_{R,T,\tau}^{(\omega_2,\varrho_2)}\right) - \vartheta R_2^{i,j}\left(x_{G,L,r}^{(\omega_1,\varrho_1)}, t_{R,T,\tau}^{(\omega_2,\varrho_2)}\right) \\ &\quad + \kappa R_3^{i,j}(x_{G,L,r}^{(\omega_1,\varrho_1)}, t_{R,T,\tau}^{(\omega_2,\varrho_2)}). \end{aligned} \tag{41}$$

Furthermore, $(N-1)$ algebraic equations are derived from the initial conditions as follows:

$$\sum_{i,j=0}^{N} a_{ij} R_0^{i,j}\left(x_{G,L,r}^{(\omega_1,\varrho_1)}, 0\right) = \varphi_1\left(x_{G,L,r}^{(\omega_1,\varrho_1)}\right), \quad r = 1,\dots,N-1, \tag{42}$$

and $(2N+2)$ equations are furnished from boundary conditions as follows:

$$\begin{cases} \sum_{i,j=0}^{N} a_{ij} R_0^{i,j}\left(0, t_{R,T,\tau}^{(\omega_2,\varrho_2)}\right) = \varphi_2\left(t_{R,T,\tau}^{(\omega_2,\varrho_2)}\right), & \tau = 0,\dots,N, \\ \sum_{i,j=0}^{N} a_{ij} R_0^{i,j}\left(L, t_{R,T,\tau}^{(\omega_2,\varrho_2)}\right) = \varphi_3\left(t_{R,T,\tau}^{(\omega_2,\varrho_2)}\right), & \tau = 0,\dots,N. \end{cases} \tag{43}$$

Mixing (40), (42), and (43), a system containing $(N+1)^2$ equations with $(N+1)^2$ unknowns will be derived. After solving the system and calculating a_{ij} coefficients, then the approximate solution of f_N in each value of (x,t) in the domain of (33) will be attained.

3.2 2D case

Here, we impose a similar algorithm to solve two-dimensional FADE (1) with initial, side criteria (2) and (3), respectively.

Now, $f(x,y,t)$ is approximated using triple SJPs as follows:

$$f_N(x,y,t) = \sum_{i,j,k=0}^{N} a_{ijk} P_{L,i}^{(\omega_1,\varrho_1)}(x) P_{I,j}^{(\omega_2,\varrho_2)}(y) P_{T,k}^{(\omega_3,\varrho_3)}(t). \tag{44}$$

The following relations are defined for summarization of the initial and side criteria and fractional derivatives of $f(x,y,t)$:

$$R_0^{i,j,k}(x,y,t) = P_{L,i}^{(\omega_1,\varrho_1)}(x) P_{I,j}^{(\omega_2,\varrho_2)}(y) P_{T,k}^{(\omega_3,\varrho_3)}(t), \tag{45}$$
$$R_1^{i,j,k}(x,y,t) = P_{L,i}^{(\omega_1,\varrho_1)}(x) P_{I,j}^{(\omega_2,\varrho_2)}(y) P_{T,k}^{(\omega_3,\varrho_3,\xi(x,y))}(t), \tag{46}$$
$$R_2^{i,j,k}(x,y,t) = P_{L,i}^{(\omega_1,\varrho_1,\eta_1(x,y,t))}(x) P_{I,j}^{(\omega_2,\varrho_2)}(y) P_{T,k}^{(\omega_3,\varrho_3)}(t), \tag{47}$$
$$R_3^{i,j,k}(x,y,t) = P_{L,i}^{(\omega_1,\varrho_1)}(x) P_{I,j}^{(\omega_2,\varrho_2,\eta_2(x,y,t))}(y) P_{T,k}^{(\omega_3,\varrho_3)}(t), \tag{48}$$
$$R_4^{i,j,k}(x,y,t) = P_{L,i}^{(\omega_1,\varrho_1,\rho_1(x,y,t))}(x) P_{I,j}^{(\omega_2,\varrho_2)}(y) P_{T,k}^{(\omega_3,\varrho_3)}(t), \tag{49}$$
$$R_5^{i,j,k}(x,y,t) = P_{L,i}^{(\omega_1,\varrho_1)}(x) P_{I,j}^{(\omega_2,\varrho_2,\rho_2(x,y,t))}(y) P_{T,k}^{(\omega_3,\varrho_3)}(t). \tag{50}$$

Substituting relation (44) in (1) and using relations (45)-(50), we have:

$$\begin{aligned}\sum_{i,j,k=0}^{N} a_{ijk} R_1^{i,j,k}(x,y,t) = {}& \vartheta\Big(\sum_{i,j,k=0}^{N} a_{ijk} R_2^{i,j,k}(x,y,t) + \sum_{i,j,k=0}^{N} a_{ijk} R_3^{i,j,k}(x,y,t)\Big) \\ & - \kappa\Big(\sum_{i,j,k=0}^{N} a_{ijk} R_4^{i,j,k}(x,y,t) + \sum_{i,j,k=0}^{N} a_{ijk} R_5^{i,j,k}(x,y,t)\Big) \\ & + S\left(\sum_{i,j,k=0}^{N} a_{ijk} R_0^{i,j,k}(x,y,t), x, y, t\right),\end{aligned} \tag{51}$$

and, numerical behavior of initial and boundary conditions is as follows:

$$\sum_{i,j,k=0}^{N} a_{ijk} R_0^{i,j,k}(x,y,0) = \varphi_1\left(x,y\right), \qquad (x,y)\in\Omega, \tag{52}$$

$$\begin{cases} \sum_{i,j,k=0}^{N} a_{ijk} R_0^{i,j,k}(0,y,t) = \varphi_2\left(0,y,t\right), & y\in[0,I], \quad t\in[0,T], \\ \sum_{i,j,k=0}^{N} a_{ijk} R_0^{i,j,k}(L,y,t) = \varphi_2\left(L,y,t\right), & y\in[0,I], \quad t\in[0,T], \\ \sum_{i,j,k=0}^{N} a_{ijk} R_0^{i,j,k}\left(x,0,t\right) = \varphi_2\left(x,0,t\right), & x\in[0,L], \quad t\in[0,T], \\ \sum_{i,j,k=0}^{N} a_{ijk} R_0^{i,j,k}(x,I,t) = \varphi_2\left(x,I,t\right), & x\in[0,L], \quad t\in[0,T]. \end{cases} \tag{53}$$

The results in $(x_{G,L,r}^{(\omega_1,\varrho_1)}, y_{G,I,s}^{(\omega_2,\varrho_2)}, t_{R,T,\tau}^{(\omega_3,\varrho_3)})$ points are examined to implement the shifted Jacobi collocation scheme in (51), (52) and (53). Here, $x_{G,L,r}^{(\omega_1,\varrho_1)}$ for any $(r=0,\dots,N)$, $y_{G,I,s}^{(\omega_2,\varrho_2)}$, for any $(s=0,\dots,N)$, and $t_{R,T,\tau}^{(\omega_3,\varrho_3)}$ for any $(\tau=1,\dots,N)$ are roots of $P_{L,N+1}^{(\omega_1,\varrho_1)}(x)$, $P_{I,N+1}^{(\omega_2,\varrho_2)}(y)$, and $P_{T,N}^{(\omega_3,\varrho_3+1)}(t)$, respectively while $t_{R,T,0}^{(\omega_3,\varrho_3)}=0$. Therefore, collocating the equations (51), (52) and (53) in collocation points $(x_{G,L,r}^{(\omega_1,\varrho_1)}$, $y_{G,I,s}^{(\omega_2,\varrho_2)}$, $t_{R,T,\tau}^{(\omega_3,\varrho_3)})$ is defined as follows:

$$\begin{aligned} &\sum_{i,j,k=0}^{N} a_{ijk} F_1^{i,j,k}(x_{G,L,r}^{(\omega_1,\varrho_1)}, y_{G,I,s}^{(\omega_2,\varrho_2)}, t_{R,T,\tau}^{(\omega_3,\varrho_3)}) \\ &= S\left(\sum_{i,j,k=0}^{N} a_{ij} R_0^{i,j}(x_{G,L,r}^{(\omega_1,\varrho_1)}, y_{G,I,s}^{(\omega_2,\varrho_2)}, t_{R,T,\tau}^{(\omega_3,\varrho_3)}), x_{G,L,r}^{(\omega_1,\varrho_1)}, y_{G,I,s}^{(\omega_2,\varrho_2)}, t_{R,T,\tau}^{(\omega_3,\varrho_3)}\right), \\ &\quad r=1,\dots,N-1, \quad s=1,\dots,N-1, \quad \tau=1,\dots,N, \end{aligned} \tag{54}$$

wherein

$$\begin{aligned} &F_1^{i,j,k}\left(x_{G,L,r}^{(\omega_1,\varrho_1)}, y_{G,I,s}^{(\omega_2,\varrho_2)}, t_{R,T,\tau}^{(\omega_3,\varrho_3)}\right) = R_1^{i,j,k}\left(x_{G,L,r}^{(\omega_1,\varrho_1)}, y_{G,I,s}^{(\omega_2,\varrho_2)}, t_{R,T,\tau}^{(\omega_3,\varrho_3)}\right) \\ &- \vartheta(R_2^{i,j,k}\left(x_{G,L,r}^{(\omega_1,\varrho_1)}, y_{G,I,s}^{(\omega_2,\varrho_2)}, t_{R,T,\tau}^{(\omega_3,\varrho_3)}\right) + R_3^{i,j,k}\left(x_{G,L,r}^{(\omega_1,\varrho_1)}, y_{G,I,s}^{(\omega_2,\varrho_2)}, t_{R,T,\tau}^{(\omega_3,\varrho_3)}\right)) \\ &+ \kappa(R_4^{i,j,k}\left(x_{G,L,r}^{(\omega_1,\varrho_1)}, y_{G,I,s}^{(\omega_2,\varrho_2)}, t_{R,T,\tau}^{(\omega_3,\varrho_3)}\right) + R_5^{i,j,k}\left(x_{G,L,r}^{(\omega_1,\varrho_1)}, y_{G,I,s}^{(\omega_2,\varrho_2)}, t_{R,T,\tau}^{(\omega_3,\varrho_3)}\right)). \end{aligned} \tag{55}$$

while the initial and boundary conditions are

$$R_0^{i,j,k}\left(x_{G,L,r}^{(\omega_1,\varrho_1)}, y_{G,I,s}^{(\omega_2,\varrho_2)}, 0\right) = \varphi_1\left(x_{G,L,r}^{(\omega_1,\varrho_1)}, y_{G,I,s}^{(\omega_2,\varrho_2)}\right), \quad r=0,\dots,N, \quad s=0,\dots,N, \tag{56}$$

$$\begin{cases} \sum_{i,j,k=0}^{N} a_{ijk} R_0^{i,j,k}(0, y_{G,I,s}^{(\omega_2,\varrho_2)}, t_{R,T,\tau}^{(\omega_3,\varrho_3)}) = \varphi_2\left(0, y_{G,I,s}^{(\omega_2,\varrho_2)}, t_{R,T,\tau}^{(\omega_3,\varrho_3)}\right), \\ \qquad s = 0, \dots, N-1, \quad \tau = 1, \dots, N, \\ \sum_{i,j,k=0}^{N} a_{ijk} R_0^{i,j,k}(L, y_{G,I,s}^{(\omega_2,\varrho_2)}, t_{R,T,\tau}^{(\omega_3,\varrho_3)}) = \varphi_2\left(L, y_{G,I,s}^{(\omega_2,\varrho_2)}, t_{R,T,\tau}^{(\omega_3,\varrho_3)}\right), \\ \qquad s = 0, \dots, N-1, \quad \tau = 1, \dots, N, \\ \sum_{i,j,k=0}^{N} a_{ijk} R_0^{i,j,k}\left(x_{G,L,r}^{(\omega_1,\varrho_1)}, 0, t_{R,T,\tau}^{(\omega_3,\varrho_3)}\right) = \varphi_2\left(x_{G,L,r}^{(\omega_1,\varrho_1)}, 0, t_{R,T,\tau}^{(\omega_3,\varrho_3)}\right), \\ \qquad r = 0, \dots, N-1, \quad \tau = 1, \dots, N, \\ \sum_{i,j,k=0}^{N} a_{ijk} R_0^{i,j,k}(x_{G,L,r}^{(\omega_1,\varrho_1)}, I, t_{R,T,\tau}^{(\omega_3,\varrho_3)}) = \varphi_2\left(x_{G,L,r}^{(\omega_1,\varrho_1)}, I, t_{R,T,\tau}^{(\omega_3,\varrho_3)}\right), \\ \qquad r = 0, \dots, N-1, \quad \tau = 1, \dots, N. \end{cases} \tag{57}$$

Now we attain a set of $(N+1)^3$ algebraic equations. After solving this system with a standard numerical method, $f_N(x, y, t)$ can be obtained in each point of the domain Ω.

4. Computational Aspects

Four computational experiments are discussed to reveal the high efficacy of the proposed approach. Findings obtained from various selections of ω and ϱ parameters in the Jacobi polynomials indicate that the method presents results of high accuracy and is comparable for all choices of ω and ϱ. In all instances, it is only needed to compute E_N in order to compare the approximated solution with the true resolution.

$$E_N(x,t) = |f(x,t) - f_N(x,t)|,$$

where $f(x,t)$ and $f_N(x,t)$ are the exact and approximated solutions in (x,t), respectively. In addition, the absolute error of L_∞ is used as follows:

$$L_\infty = max\{E_N(x,T) : x \in [0, L]\},$$

Example 4.1. *Suppose the following 1D FADE:*

$$D_t^{\xi(x)} f(x,t) = 2\,{}_0^R D_x^{\eta(x,t)} f(x,t) - {}_0^R D_x^{\rho(x,t)} f(x,t) + S(x,t), \qquad (x,t) \in \Omega = [0,1] \times [0,1], \tag{58}$$

with the following initial and side criteria:

$$\begin{cases} f(x,0) = 5\left(x^2 - x^3\right), & 0 \le x \le 1, \\ f(0,t) = f(1,t) = 0, & 0 \le t \le 1. \end{cases} \tag{59}$$

Also, $S(x,t)$ in (58) is defined by:

$$S(x,t)=\frac{10x^2(1-x)\,t^{2-\xi(x)}}{\Gamma(3-\xi(x))}-10(t^2+1)\left[\frac{2x^{2-\eta(x,t)}}{\Gamma(3-\eta(x,t))}-\frac{6x^{3-\eta(x,t)}}{\Gamma(4-\eta(x,t))}\right]$$
$$+5(t^2+1)\left[\frac{2x^{2-\rho(x,t)}}{\Gamma(3-\rho(x,t))}-\frac{6x^{3-\rho(x,t)}}{\Gamma(4-\rho(x,t))}\right].$$

where

$$\xi(x)=1-0.5e^{-x}, \tag{60}$$

$$\eta(x,t)=1.7+0.5e^{-\frac{x^2}{1000}-\frac{t}{50}-1}, \tag{61}$$

$$\rho(x,t)=0.7+0.5e^{-\frac{x^2}{1000}-\frac{t}{50}-1}. \tag{62}$$

The exact solution is $f(x,t)=5\left(t^2+1\right)x^2(1-x)$, Zhang et al. (2014).

Results obtained from computational evidences of the problem have been brought in Table 1. Using the algorithm presented in Section 3 for $N=6$, we will furnish $f_N(x,t)$. As shown in Table 1, for various parameters of ω and ϱ, the absolute error in various points in interval of [0,1] has been furnished. At the end, the numerical results have been compared with the findings of Zhang et al. (2014). Zhang uses finite difference method (FDM) to solve this equation. Using FDM with 150 points, an error of 10^{-3} will be furnished; however, utilizing Jacobi collocation method with 6 points, a highly accurate solution is furnished which its error is near 10^{-16}.

Table 1: Point to point error furnished through implementing Jacobi collocation method in Example 4.1 by $N=6$ and its comparison to FDMZhang et al. (2014) in N=150

	Jacobi Collocation Method				FDM
x	$\omega_1=\varrho_1=0$ $\omega_2=\varrho_2=0$	$\omega_1=\varrho_1=0.5$ $\omega_2=\varrho_2=0.5$	$-\omega_1=\varrho_1=0.5$ $-\omega_2=\varrho_2=0.5$	$\omega_1=1,\varrho_1=0$ $\omega_2=0,\varrho_2=1$	$N=150$
0	5.5511e-17	1.1102e-15	6.6613e-16	1.1102e-16	1.0001e-03
0.1	9.7145e-17	4.5797e-16	5.4123e-16	9.7145e-17	1.0492e-03
0.2	2.7756e-16	2.2204e-16	2.2204e-16	2.7756e-16	2.0690e-03
0.3	3.3307e-16	1.1102e-16	2.2204e-16	1.1102e-16	3.0214e-03
0.4	5.5511e-16	6.6613e-16	0	4.4409e-16	3.8254e-03
0.5	4.4409e-16	2.2204e-16	0	4.4409e-16	4.3921e-03
0.6	8.8818e-16	4.4409e-16	4.4409e-16	6.6613e-16	4.6258e-03
0.7	4.4409e-16	6.6613e-16	1.1102e-15	4.4409e-16	4.4228e-03
0.8	6.6613e-16	8.8818e-16	4.4409e-16	2.2204e-16	3.6700e-03
0.9	8.8818e-16	5.5511e-16	6.6613e-16	0	2.2424e-03
1	2.2204e-16	4.4409e-16	1.1102e-16	8.8818e-16	1.2354e-03

In Figure 1, we illustrated the curves of the exact and approximated solutions of (58) at $t = 0.4, 0.6, 0.8, 1$. Figure 2 shows the numerical solution in 3D case. Figures 3 and 4 show the absolute error in one point and a fixed time, respectively. All the figures are based on $N = 6$ and $\omega_1 = \omega_2 = \varrho_1 = \varrho_2 = 0$. In figure 5, the absolute error of example 4.1 is plotted for different values of the fractional order of derivatives. This figure shows that when the fractional derivatives order approach to their integer values $(\xi, \rho \to 1, \eta \to 2)$, the absolute error also decreases substantially. Here the vertical axis represents the absolute error of the approximate solution and the horizontal axis corresponds to the parameter r:

$$r = 1 - norm(1 - \xi, 2 - \eta, 1 - \rho). \tag{63}$$

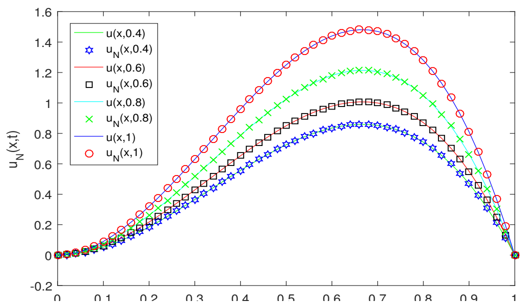

Figure 1: Comparison of the approximated and exact solutions of Example 4.1 in various timesfor $N = 6$ and $\omega_1{=}\omega_2{=}\varrho_1{=}\varrho_2 = 0$.

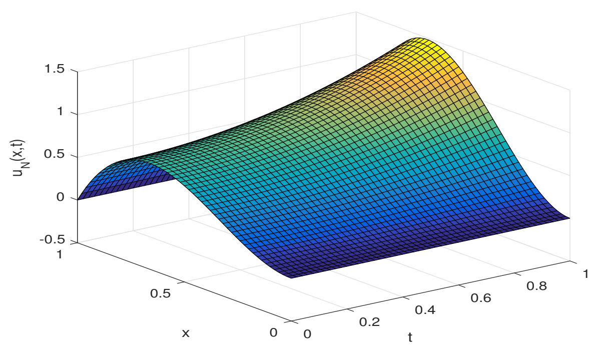

Figure 2: Numerical solution of Example 4.1 in 3D state for $N = 6$ and $\omega_1{=}\omega_2{=}\varrho_1{=}\varrho_2 = 0$.

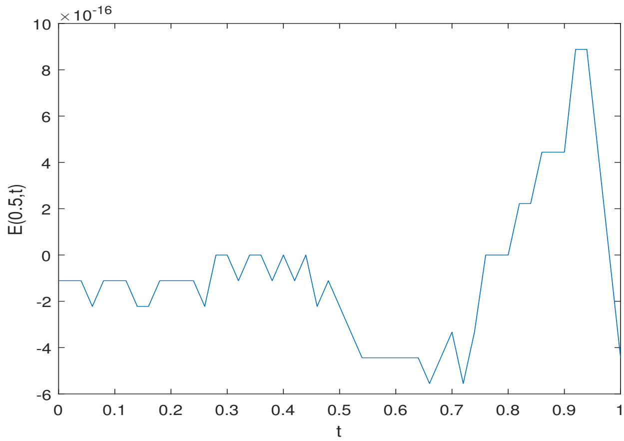

Figure 3: Absolute error of Example 4.1 in $(0.5, t)$ point for $N = 6$ and $\omega_1{=}\omega_2{=}\varrho_1{=}\varrho_2 = 0$.

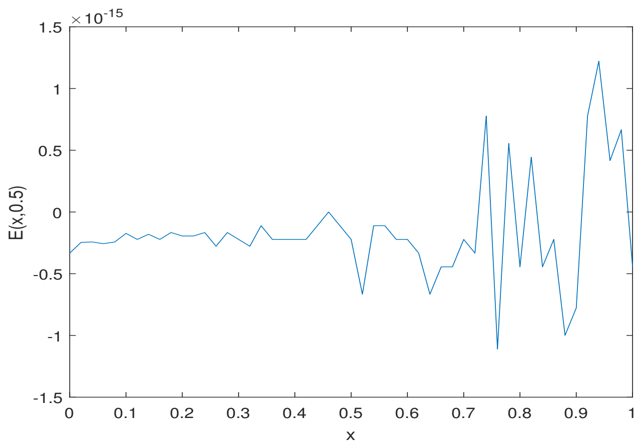

Figure 4: Absolute error of Example 4.1 in $(x, 0.5)$ point for $N = 6$ and $\omega_1{=}\omega_2{=}\varrho_1{=}\varrho_2 = 0$.

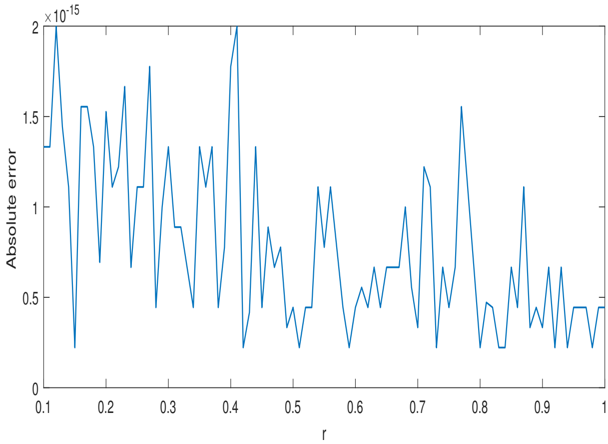

Figure 5: The absolute error of example 4.1 when the fractional order of derivatives tends to their integer values (ω_1=ω_2=ϱ_1=ϱ_2 = 0)

Example 4.2. *Let us solve the following 1D FADE:*

$$D_t^{\xi(x)} f(x,t) = 2\,{}_0^R D_x^{\eta(x,t)} f(x,t) - {}_0^R D_x^{\rho(x,t)} f(x,t) + S(x,t), \qquad (x,t) \in \Omega = [0, 2\pi] \times [0,1], \tag{64}$$

with the following boundary and initial conditions:

$$\begin{cases} f(x,0) = \sin(x), & 0 \le x \le 2\pi, \\ f(0,t) = f(2\pi,t) = 0, & 0 \le t \le 1, \end{cases} \tag{65}$$

and

$$S(x,t) = \sin(x) \sum_{n=1}^{\infty} \frac{(-1)^n t^{2n-\xi(x)}}{\Gamma(2n+1-\xi(x))} - 2\cos(t) \sum_{n=0}^{\infty} \frac{(-1)^n x^{2n+1-\eta(x,t)}}{\Gamma(2n+2-\eta(x,t))} + \cos(t) \sum_{n=0}^{\infty} \frac{(-1)^n x^{2n+1-\rho(x,t)}}{\Gamma(2n+2-\rho(x,t))}, \tag{66}$$

where ξ, η, ρ are valued based on three following categories:

case $1:\ \xi(x) = 0.8 + 0.01\ln(5x),\ \eta(x,t) = 1.8 + 0.01x^2t^2,\ \rho(x,t) = 0.8 + 0.01x^2\mathrm{sint}$,

case $2:\ \xi(x) = 0.8,\ \eta(x,t) = 1.8,\ \rho(x,t) = 0.8,$

case $3:\ \xi(x) = \cos(\frac{x}{2\pi}+0.1),\ \eta(x,t) = 2 - (\sin^2(t\cos^2(x) + 0.1),\ \rho(x,t) = \frac{e^{xt}}{1000}.$

Exact solution is given by $f(x,t) = \sin(x)\cos(t)$.

Results of this problem have been presented in Tables 2 and 3. As shown in Table 2, the absolute errors for ξ, η, ρ in case (1) and various parameters of ω , ϱ and $N = 8, 10, 12, 14, 16, 18$ have been compared with each other. Finally, the findings obtained through the Jacobi collocation method have been compared to the FDM results Zhang et al. (2014). Table 3 presents the absolute error for different order derivatives in various points.

Regarding the findings in Tables 2 and 3, comparing to other approaches including the FDM Zhang et al. (2014), it could be observed that the scheme is efficient with finite number of points. Figure 6 reveals a comparison of the exact and approximated solutions. In Figure 7, numerical solution has been shown for various times in the 3D case. All the figures are drawn for $N = 18$, $\omega_1 = \omega_2 = \varrho_1 = \varrho_2 = 0$ and case (1). In figure 8, the absolute error of example 4.2 is plotted for different values of the fractional order of derivatives.

Table 2: Absolute error obtained through implementing Jacobi collocation method in Example 4.2 in various points with derivative of ξ, η, ρ order in case (1) and its comparison to FDM Zhang et al. (2014).

	Jacobi Collocation Method				FDM
N	$\omega_1 = \varrho_1 = 0$ $\omega_2 = \varrho_2 = 0$	$\omega_1 = \varrho_1 = 0.5$ $\omega_2 = \varrho_2 = 0.5$	$-\omega_1 = \varrho_1 = 0.5$ $-\omega_2 = \varrho_2 = 0.5$	$\omega_1 = 1, \varrho_1 = 0$ $\omega_2 = 0, \varrho_2 = 1$	-
8	4.6698e-04	8.8157e-04	1.1440e-03	2.5695e-03	7.9725e-02
10	1.3348e-05	2.7840e-05	3.1508e-05	9.0421e-05	6.5264e-02
12	2.4776e-07	5.6105e-07	5.8426e-07	1.9879e-06	5.4834e-02
14	3.2778e-09	7.9674e-09	7.8259e-09	3.0277e-08	4.7195e-02
16	3.1670e-11	8.6281e-11	7.9408e-11	3.4125e-10	4.1679e-02
18	4.6937e-13	5.1170e-13	6.2958e-13	2.6182e-12	3.7263e-02

Table 3: Comparison of the absolute error obtained in Example 4.2 in various points with derivatives of fixed or variable order for $\omega_1 = \omega_2 = \varrho_1 = \varrho_2 = 0$

Order	**N=8**	**N=10**	**N=12**	**N=14**	**N=16**	**N=18**
case 1	4.6698e-04	1.3348e-05	2.4776e-07	3.2778e-09	3.1670e-11	4.6937e-13
case 2	8.0552e-04	2.4998e-05	4.9999e-07	7.0729e-09	7.3890e-11	7.6700e-13
case 3	1.2082e-03	4.2078e-05	9.3519e-07	1.4175e-08	1.5777e-10	1.5018e-12

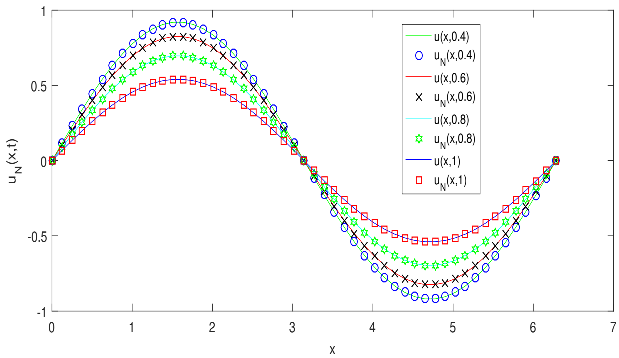

Figure 6: Comparison of the approximated and true solutions of Example 4.2 in various times for $N = 18$, $\omega_1 = \omega_2 = \varrho_1 = \varrho_2 = 0$ and case (1).

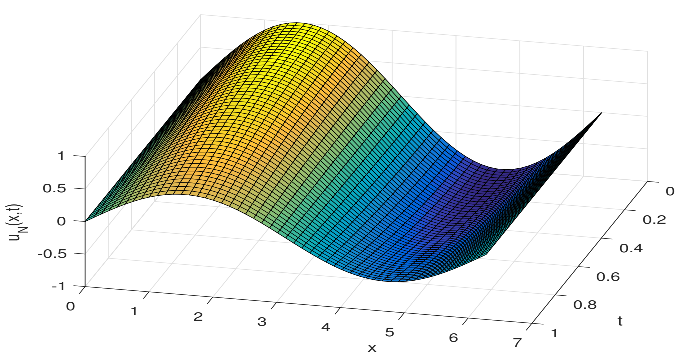

Figure 7: Computational behavior in Example 4.2 in the 3D case for $N = 18$, $\omega_1 = \omega_2 = \varrho_1 = \varrho_2 = 0$ and ξ_1, η_1, ρ_1.

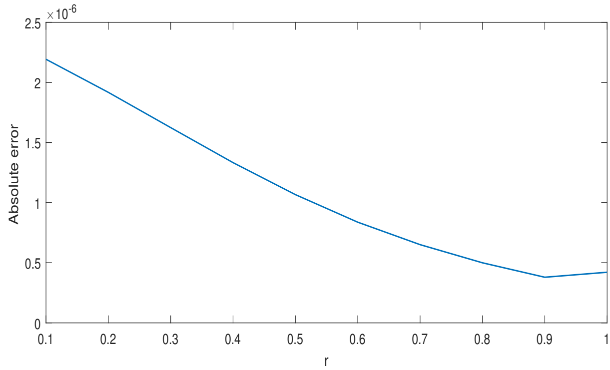

Figure 8: The absolute error of example 4.2 when the fractional order of derivatives tends to their integer values (ω_1=ω_2=ϱ_1=ϱ_2 = 0)

Example 4.3. *Consider the following two-dimensional FADE*

$$D_t^{\xi(x,y)} f(x,y,t) = 2({}_0^R D_x^{\eta_1(x,y,t)} f(x,y,t) + {}_0^R D_y^{\eta_2(x,y,t)} f(x,y,t)) + S(x,y,t),$$
$$(x,y,t) \in [0,1] \times [0,1] \times [0,1], \tag{67}$$

where

$$S(x,y,t) = \frac{2t^{2-\xi(x,y)}x^2y^2}{\Gamma(3-\xi(x,y))} - 4t^2(\frac{x^{2-\eta_1(x,y,t)}y^2}{\Gamma(3-\eta_1(x,y,t))} + \frac{x^2y^{2-\eta_2(x,y,t)}}{\Gamma(3-\eta_2(x,y,t))}). \tag{68}$$

Initial and boundary conditions are selected so that the exact solution is as follows:

$$f(x,y,t) = t^2x^2y^2, \tag{69}$$

In addition, the orders of fractional derivatives are valued based on three following categories:

$$case1: \ \xi(x) = 0.8, \ \eta_1(x,t) = 1.8, \ \eta_2(x,t) = 1.8,$$
$$case2: \ \xi(x) = 0.5 + \frac{xy}{5}, \ \eta_1(x,t) = 0.2 + \sqrt{1+\sinh(xyt)},$$
$$\eta_2(x,t) = 0.5 + \sqrt{1+\tanh(xyt)},$$
$$case3: \ \xi(x) = 0.5 + \frac{xy}{5}, \ \eta_1(x,t) = 0.2 + \sqrt{1+\sinh(xyt)}, \ \eta_2(x,t) = 1.8.$$

The mentioned algorithm in subsection 3.2 is applied to tackle this problem. The results have been presented in Table 4 for $N = 4$ and $N = 6$. In this table, absolute error is furnished for various order derivatives and different parameters of ω and ϱ. In Figure 9, the approximated solution at $t = 1$ is presented for parameters of $-\omega_1 = -\varrho_1 = \omega_2 = \varrho_2 = \omega_3 = \varrho_3 = 0.5$, and the case (2). In figure 10, the absolute error of example 4.3 is plotted for different values of the fractional order of derivatives.

Table 4: Absolute error obtained through implementing Jacobi collocation method in Example 4.3 with $N = 4, 6$ for variable and fixed fractional order derivative.

N=4				
Order	$\omega_1 = \varrho_1 = 0$ $\omega_2 = \varrho_2 = 0$ $\omega_3 = \varrho_3 = 0$	$\omega_1 = \varrho_1 = -0.5$ $\omega_2 = \varrho_2 = 0$ $\omega_3 = \varrho_3 = 0$	$\omega_1 = \varrho_1 = -0.5$ $\omega_2 = \varrho_2 = 0.5$ $\omega_3 = \varrho_3 = 0.5$	$\omega_1 = \varrho_1 = -0.5$ $\omega_2 = \varrho_2 = -0.5$ $\omega_3 = \varrho_3 = -0.5$
case 1	3.2240e-09	2.7902e-09	1.1239e-09	7.7602e-16
case 2	3.7630e-09	2.7902e-09	1.3399e-09	6.0883e-16
case 3	4.0157e-09	2.7902e-09	1.3350e-09	5.7067e-09
N=6				
Order	$\omega_1 = \varrho_1 = 0$ $\omega_2 = \varrho_2 = 0$ $\omega_3 = \varrho_3 = 0$	$\omega_1 = \varrho_1 = -0.5$ $\omega_2 = \varrho_2 = 0$ $\omega_3 = \varrho_3 = 0$	$\omega_1 = \varrho_1 = -0.5$ $\omega_2 = \varrho_2 = 0.5$ $\omega_3 = \varrho_3 = 0.5$	$\omega_1 = \varrho_1 = -0.5$ $\omega_2 = \varrho_2 = -0.5$ $\omega_3 = \varrho_3 = -0.5$
case 1	2.4023e-15	6.3005e-16	9.3114e-16	7.7896e-16
case 2	3.1850e-09	8.8243e-09	6.8032e-16	9.4015e-16
case 3	3.1850e-09	1.2154e-15	8.0023e-16	1.5399e-15

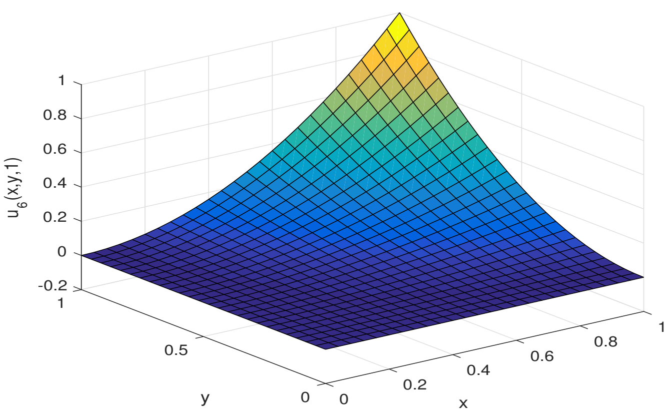

Figure 9: Computational solution of Example 4.3 at $t = 1$ for $N = 6$, $-\omega_1 = -\varrho_1 = \omega_2 = \varrho_2 = \omega_3 = \varrho_3 = 0.5$ and case (2).

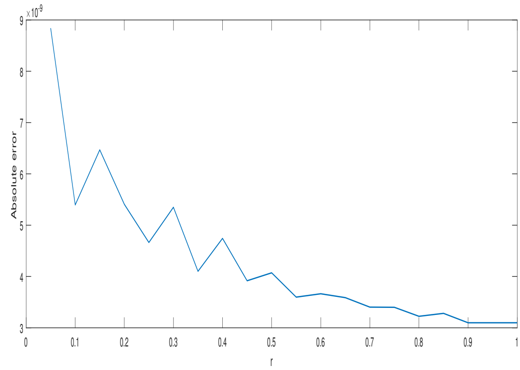

Figure 10: The absolute error of example 4.3 when the fractional order of derivatives tends to their integer values ($\omega_1 = \varrho_1 = \omega_2 = \varrho_2 = \omega_3 = \varrho_3 = 0$)

Example 4.4. *Here, we take into account the following equation:*

$$\begin{aligned} D_t^{\xi(x,y)} f(x,y,t) = {} & ({}_0^R D_x^{\eta_1(x,y,t)} f(x,y,t) + {}_0^R D_y^{\eta_2(x,y,t)} f(x,y,t)) \\ & - (({}_0^R D_x^{\rho_1(x,y,t)} f(x,y,t) + {}_0^R D_y^{\rho_2(x,y,t)} f(x,y,t))) + S(x,y,t), \\ & (x,y,t) \in [0,1] \times [0,1] \times [0,1], \end{aligned} \tag{70}$$

where

$$\begin{aligned} S(x,t) = {} & \frac{10x^2y^2(1-x)(1-y)\,t^{1-\xi(x)}}{\Gamma(2-\xi(x))} \\ & - 10(t+1)(1-y)y^2 \left[\frac{2x^{2-\eta_1(x,t)}}{\Gamma(3-\eta_1(x,t))} - \frac{6x^{3-\eta_1(x,t)}}{\Gamma(4-\eta_1(x,t))}\right] \\ & + 10(t+1)(1-y)y^2 \left[\frac{2x^{2-\rho_1(x,t)}}{\Gamma(3-\rho_1(x,t))} - \frac{6x^{3-\rho_1(x,t)}}{\Gamma(4-\rho_1(x,t))}\right] \\ & - 10(t+1)(1-x)x^2 \left[\frac{2y^{2-\eta_2(x,t)}}{\Gamma(3-\eta_2(x,t))} - \frac{6y^{3-\eta_2(x,t)}}{\Gamma(4-\eta_2(x,t))}\right] \\ & + 10(t+1)(1-x)x^2 \left[\frac{2y^{2-\rho_2(x,t)}}{\Gamma(3-\rho_2(x,t))} - \frac{6y^{3-\rho_2(x,t)}}{\Gamma(4-\rho_2(x,t))}\right]. \end{aligned} \tag{71}$$

In addition, the orders of fractional derivatives are valued based on three following categories:

$case1: \ \xi(x) = 0.8, \ \eta_1(x,t) = 1.8, \ \eta_2(x,t) = 1.2, \ \rho_1(x,t) = 0.9, \ \rho_2(x,t) = 0.3,$

$case2: \ \xi(x) = \sqrt{0.1 + \frac{xy+y}{5}}, \ \eta_1(x,t) = 0.1 + (1 + tanh(xyt)),$

$\eta_2(x,t) = \frac{11 + xy + yt}{10}, \ \rho_1(x,t) = 0.1 + sin(xyt), \ \rho_2(x,t) = (0.1 + sin(xyt))^2,$

$case3: \ \xi(x) = \sqrt{0.1 + \frac{xy+y}{5}}, \ \eta_1(x,t) = 0.1 + (1 + tanh(xyt)), \ \eta_2(x,t) = 1.2,$

$\rho_1(x,t) = 0.1 + sin(xyt), \ \rho_2(x,t) = 0.3.$

Initial and boundary conditions are selected so that the exact solution is as follows:

$$f(x,y,t) = 10(t+1)(xy)^2(1-x)(1-y). \tag{72}$$

The obtained results for $N = 4$ and $N = 8$ at $t = 1$ and for various parameters of ω and ϱ have been shown in Table 5. It is tried to furnish and compare the absolute error for various values of derivatives of fixed or variable orders. As it can be seen, by using considerably small number of points and finite collocation points, the best results can be obtained, which shows high efficacy of the scheme. In Figure 11, the approximated solution of Example 4.4 have been shown at $t = 1$ for parameters of $\omega_1 = \varrho_1 = \omega_2 = \varrho_2 = \omega_3 = \varrho_3 = -0.5$ and case (2). In figure 12, the absolute error of example 4.4 is plotted for different values of the fractional order of derivatives.

Table 5: The absolute error furnished through Jacobi collocation method in Example 4.4 with $N = 4, 8$ for fixed and variable fractional order derivatives.

		N=4		
Order	$\omega_1 = \varrho_1 = 0$ $\omega_2 = \varrho_2 = 0$ $\omega_3 = \varrho_3 = 0$	$\omega_1 = \varrho_1 = -0.5$ $\omega_2 = \varrho_2 = 0$ $\omega_3 = \varrho_3 = 0$	$\omega_1 = \varrho_1 = -0.5$ $\omega_2 = \varrho_2 = 0.5$ $\omega_3 = \varrho_3 = 0.5$	$\omega_1 = \varrho_1 = -0.5$ $\omega_2 = \varrho_2 = -0.5$ $\omega_3 = \varrho_3 = -0.5$
*case*1	1.5104e-10	1.0065e-09	7.1329e-10	1.3359e-09
*case*2	5.0066e-10	7.1728e-10	5.4320e-10	1.2884e-09
*case*3	3.1525e-10	5.7889e-10	5.6960e-10	1.8027e-09
		N=8		
Order	$\omega_1 = \varrho_1 = 0$ $\omega_2 = \varrho_2 = 0$ $\omega_3 = \varrho_3 = 0$	$\omega_1 = \varrho_1 = -0.5$ $\omega_2 = \varrho_2 = 0$ $\omega_3 = \varrho_3 = 0$	$\omega_1 = \varrho_1 = -0.5$ $\omega_2 = \varrho_2 = 0.5$ $\omega_3 = \varrho_3 = 0.5$	$\omega_1 = \varrho_1 = -0.5$ $\omega_2 = \varrho_2 = -0.5$ $\omega_3 = \varrho_3 = -0.5$
*case*1	8.7174e-16	1.9361e-15	2.1672e-15	1.9468e-15
*case*2	1.4861e-15	5.5106e-10	2.6045e-15	2.9432e-15
*case*3	9.2311e-10	2.9177e-15	2.7667e-15	2.9946e-15

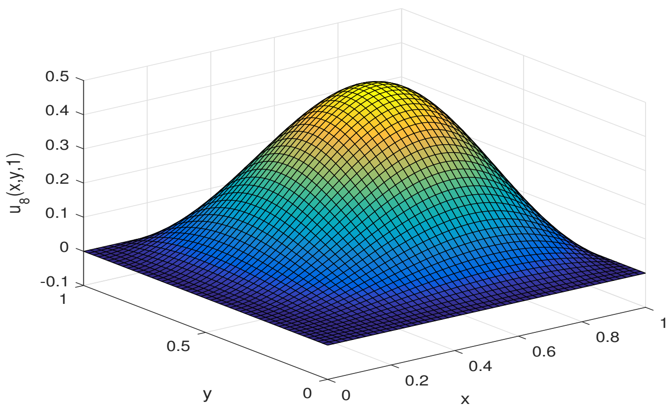

Figure 11: Numerical solution of Example 4.4 at t=1 for N=8 and case (2), $\omega_1 = \varrho_1 = \omega_2 = \varrho_2 = \omega_3 = \varrho_3 = -0.5$

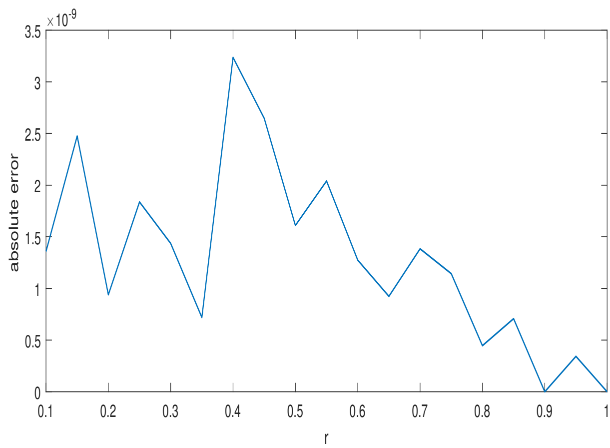

Figure 12: The absolute error of example 4.4 when the fractional order of derivatives tends to their integer values ($\omega_1 = \varrho_1 = \omega_2 = \varrho_2 = \omega_3 = \varrho_3 = -0.5$)

5. Conclusions

A spectral collocation method was used in this article to furnish the numerical solution of variable order FADE in 1D and 2D cases. The solution of advection-dispersion equation is approximated using the Jacobi functions, which are considered as the basic functions, and the collocation points are chosen from SJ-GR-c and SJ-G-c interpolation points for time and space variables, respectively. Finally, using this collocation method, a system of algebraic equations would be furnished which had been solved with a standard computational method. Numerical solutions obtained in the last section indicated that this method has considerably high accuracy compared to the other existing methods such as the FDM approach.

References

Ahmadian, A., Ismail, F., Salahshour, S., Baleanu, D., and Ghaemi, F. (2017). Uncertain viscoelastic models with fractional order: A new spectral tau method to study the numerical simulations of the solution. *Communications in Nonlinear Science and Numerical Simulation*, 53:44–64.

Ahmadian, A., Salahshour, S., and Chan, C. S. (2016). Fractional differential systems: a fuzzy solution based on operational matrix of shifted chebyshev polynomials and its applications. *IEEE Transactions on Fuzzy Systems*, 25(1):218–236.

Askey, R. (1975). *Orthogonal polynomials and special functions*, volume 21. Siam.

Atabakan, Z. P., Nasab, A. K., and Kilicman, A. (2014). Spectral homotopy analysis method for solving nonlinear volterra integro differential equations. *Malaysian Journal of Mathematical Sciences*, 8:153–161.

Bhrawy, A. and Zaky, M. (2015). Numerical simulation for two-dimensional variable-order fractional nonlinear cable equation. *Nonlinear Dynamics*, 80(1-2):101–116.

Bhrawy, A. H. and Alghamdi, M. A. (2012). A shifted jacobi-gauss-lobatto collocation method for solving nonlinear fractional langevin equation involving two fractional orders in different intervals. *Boundary Value Problems*, 2012(1):62.

Bhrawy, A. H., Alzaidy, J. F., Abdelkawy, M. A., and Biswas, A. (2016a). Jacobi spectral collocation approximation for multi-dimensional time-fractional schrödinger equations. *Nonlinear Dynamics*, 84(3):1553–1567.

Bhrawy, A. H., Mallawi, F., and Abdelkawy, M. A. (2016b). New spectral collocation algorithms for one-and two-dimensional schrödinger equations with a kerr law nonlinearity. *Advances in Difference Equations*, 2016(1):18.

Bhrawy, A. H., Taha, T. M., and Machado, J. A. T. (2015). A review of operational matrices and spectral techniques for fractional calculus. *Nonlinear Dynamics*, 81(3):1023–1052.

Canuto, C., Hussaini, M. Y., Quarteroni, A., and Zang, T. A. (2006). *Spectral methods*. Springer.

Carella, A. R. and Dorao, C. A. (2013). Least-squares spectral method for the solution of a fractional advection–dispersion equation. *Journal of Computational Physics*, 232(1):33–45.

Chatwin, P. and Allen, C. (1985). Mathematical models of dispersion in rivers and estuaries. *Annual Review of Fluid Mechanics*, 17(1):119–149.

Chaudhry, M. H., Cass, D. E., and Edinger, J. E. (1983). Modeling of unsteady-flow water temperatures. *Journal of Hydraulic Engineering*, 109(5):657–669.

Chen, S., Liu, F., and Burrage, K. (2014). Numerical simulation of a new two-dimensional variable-order fractional percolation equation in non-homogeneous porous media. *Computers & Mathematics with Applications*, 68(12):2133–2141.

Clavero, C., Jorge, J., and Lisbona, F. (2003). A uniformly convergent scheme on a nonuniform mesh for convection–diffusion parabolic problems. *Journal of Computational and Applied Mathematics*, 154(2):415–429.

Coimbra, C. F. (2003). Mechanics with variable-order differential operators. *Annalen der Physik*, 12(11-12):692–703.

Diethelm, K. (2010). *The analysis of fractional differential equations: An application-oriented exposition using differential operators of Caputo type*. Springer Science & Business Media.

Ervin, V. J. and Roop, J. P. (2006). Variational formulation for the stationary fractional advection dispersion equation. *Numerical Methods for Partial Differential Equations: An International Journal*, 22(3):558–576.

Eslahchi, M., Dehghan, M., and Parvizi, M. (2014). Application of the collocation method for solving nonlinear fractional integro-differential equations. *Journal of Computational and Applied Mathematics*, 257:105–128.

Gómez-Aguilar, J. (2018). Novel analytical solutions of the fractional drude model. *Optik*, 168:728–740.

Guvanasen, V. and Volker, R. (1983). Numerical solutions for solute transport in unconfined aquifers. *International Journal for Numerical Methods in Fluids*, 3(2):103–123.

Hejazi, H., Moroney, T., and Liu, F. (2014). Stability and convergence of a finite volume method for the space fractional advection–dispersion equation. *Journal of Computational and Applied Mathematics*, 255:684–697.

Hosseini, K., Bekir, A., and Ansari, R. (2017). New exact solutions of the conformable time-fractional cahn–allen and cahn–hilliard equations using the modified kudryashov method. *Optik*, 132:203–209.

Isenberg, J. and Gutfinger, C. (1973). Heat transfer to a draining film. *International Journal of Heat and Mass Transfer*, 16(2):505–512.

Kumar, N. (1983). Unsteady flow against dispersion in finite porous media. *Journal of Hydrology*, 63(3-4):345–358.

Liu, F., Zhuang, P., Anh, V., Turner, I., and Burrage, K. (2007). Stability and convergence of the difference methods for the space–time fractional advection–diffusion equation. *Applied Mathematics and Computation*, 191(1):12–20.

Magin, R. L. (2006). *Fractional calculus in bioengineering*. Begell House Redding.

Meerschaert, M. M. and Tadjeran, C. (2004). Finite difference approximations for fractional advection–dispersion flow equations. *Journal of Computational and Applied Mathematics*, 172(1):65–77.

Ortega, A., Rosales, J., Martínez, L., and Carreño, C. (2018). Fractional optical properties of drude model. *Optik*, 161:244–249.

Pandey, R. K., Singh, O. P., and Baranwal, V. K. (2011). An analytic algorithm for the space–time fractional advection–dispersion equation. *Computer Physics Communications*, 182(5):1134–1144.

Parlange, J. (1980). Water transport in soils. *Annual Review of Fluid Mechanics*, 12(1):77–102.

Sakar, F. and Güney, H. (2017). Faber polynomial coefficient estimates for subclasses of m-fold symmetric bi-univalent functions defined by fractional derivative. *Malaysian Journal of Mathematical Sciences*, 11:275–287.

Schumer, R., Benson, D. A., Meerschaert, M. M., and Wheatcraft, S. W. (2001). Eulerian derivation of the fractional advection–dispersion equation. *Journal of contaminant hydrology*, 48(1-2):69–88.

Sontakke, B., Shaik, A., and Nisar, K. (2018). Approximate solutions of a generalized hirota–satsuma coupled kdv and a coupled mkdv systems with time fractional derivatives. *Malaysian Journal of Mathematical Sciences*, 12(2):175–196.

Sun, H., Chen, W., and Chen, Y. (2009). Variable-order fractional differential operators in anomalous diffusion modeling. *Physica A: Statistical Mechanics and its Applications*, 388(21):4586–4592.

Sun, H., Chen, W., Li, C., and Chen, Y. (2012). Finite difference schemes for variable-order time fractional diffusion equation. *International Journal of Bifurcation and Chaos*, 22(04):1250085.

Szeg, G. (1939). *Orthogonal polynomials*, volume 23. American Mathematical Soc.

Tseng, C.-C. (2006). Design of variable and adaptive fractional order fir differentiators. *Signal Processing*, 86(10):2554–2566.

Ünal, E. and Gökdoğan, A. (2017). Solution of conformable fractional ordinary differential equations via differential transform method. *Optik*, 128:264–273.

Zhang, H., Liu, F., Zhuang, P., Turner, I., and Anh, V. (2014). Numerical analysis of a new space–time variable fractional order advection–dispersion equation. *Applied Mathematics and Computation*, 242:541–550.

Zhang, X., Lv, M., Crawford, J. W., and Young, I. M. (2007). The impact of boundary on the fractional advection–dispersion equation for solute transport in soil: Defining the fractional dispersive flux with the Caputo derivatives. *Advances in Water Resources*, 30(5):1205–1217.

Zheng, G. and Wei, T. (2010). Spectral regularization method for a cauchy problem of the time fractional advection–dispersion equation. *Journal of Computational and Applied Mathematics*, 233(10):2631–2640.

Zhuang, P., Liu, F., Anh, V., and Turner, I. (2009). Numerical methods for the variable-order fractional advection-diffusion equation with a nonlinear source term. *SIAM Journal on Numerical Analysis*, 47(3):1760–1781.